京 都 大 学 防 災 研 究 所 年 報 第47号 C 平成16年3月
Annuals of Disas. Prev. Res. Inst., Kyoto Univ., No. 47 C, 2004

Geo-disaster Prediction and Geo-hazard Mapping in Urban and Surrounding Areas

Susumu IAI, Shinya INAZUMI*, Masahiro CHIGIRA, Toshitaka KAMAI,
Roy, C. SIDLE, Mamoru MIMURA, Hiroshi SUWA, Takashi SAITO,
and Tetsuo TOBITA

* Graduate School of Engineering, Department of Urban Management, Kyoto University
(formerly, COE researcher, DPRI, Kyoto University)

Synopsis

Urban development rapidly expanding from lowland to surrounding hills and mountains poses increasing risks in geo-hazards, including liquefaction during earthquakes, and failure of artificial and natural slopes. Objective of this study is to develop methodologies for assessing vulnerability to these hazards, and technologies for improving the performance of geotechnical works in urban areas. This paper summarizes the results of the study with respect to (1) performance of retaining walls at waste fill in waterfront areas, (2) hazard mapping of natural slope failures through monitoring using laser scanners, and (3) hazard assessment of residential areas in valley fills and hills.

Keywords: environment, geo-disasters, hazard mapping, hills, mountains

1. Introduction

Urban areas were highly developed in lowland and rapidly expanding toward surrounding hills and mountains. The rapid expansion causes increasing hazards associated with geological and geotechnical process. In particular, liquefaction during earthquakes causes potential risks to infrastructures in urban areas. Failure of artificial and natural slopes poses potential threats to residents and communities. Objective of this study is to develop methodologies for assessing vulnerability to these hazards, and to propose techniques for improving the performance of geotechnical works in urban areas.

This paper summarizes the results focusing on the following priority issues.

(1) Waste fills in waterfront areas have been rapidly expanding and pose new threats due to failure or mal-function of retaining walls. Vulnerability of these retaining walls against waves, tsunamis, and earthquakes should be appropriately evaluated and new techniques for improving the performance of these walls should be proposed.

(2) Prediction of shallow landslides was difficult because of site-by-site variations in geotechnical conditions. However, occurrence of shallow landslides is widespread, and poses a serious threat to residents and communities in the area. A new methodology should be developed for assessing susceptibility of shallow landslides to mitigate landslide hazard.

(3) Valley fills and artificial slopes have been increasing for developing new residential areas conveniently located to large cities. Slope failures in these valley fills and hills pose immediate threats to residents. Study should be performed on these aspects of geo-hazards.

2. Performance of steel pipe sheet piles in coastal landfill site

2.1 Introduction

Due to strict environmental requirements and difficulties in land expropriation in Japan for inland landfill construction, coastal waste disposal landfills are increasingly being adopted and require large scale reclamations in ports and harbors near urban areas. In design of vertical cutoff barriers, conservation of port and harbor area as well as quality of waste material is considered. The cutoff must have both mechanical strength and low hydraulic conductivity in order to curb leakage of leachate from contained waste material to the open sea. Tokyo metropolitan city, for instance, disposes 84.7% of its waste into coastal waste disposal facilities in the sea and man-made islands. Coastal waste disposal facilities are in three designs: (a) rubble mound seawall, (b) caisson wall, and (c) double wall cutoff steel pipe sheet piles (SPSP), as shown in Fig. 1. The rubble mound is mainly for stable (non-toxic) waste material but can suffer loss of riprap which leads to erosion of the toe by wave action and requires a large area since it must slope gently for stability purposes. Caisson type is for toxic waste materials; however, caisson has a shallow penetration depth. SPSP has good penetration depth, cheap and easy to construct as a cutoff barrier in coastal waste disposal landfills, but at the current state, there is a high risk of leakage of the leachate from contained waste through traditional SPSP joints. Traditional joints in SPSP include L-T, P-P, and P-T joints as shown in Fig. 2; among their shortcomings are as follows:

(1) The joints must be grouted with mortar for sealing and increasing strength of the joint. The grouting process causes pollution leading to environmental degradation.
(2) In the current practice, mortar is pumped into the joints after installation of SPSP is complete; in this construction procedure, it is difficult to control the quality of grouting, hence, existence of uncertainty with regard to effectiveness of such treatment.
(3) Further, since the joints are submerged in a water body, injected mortar is packed to prevent segregation and the eventual dilution by the surrounding water body; this procedure increases the hydraulic conductivity of the grouted joints.
(4) Excessive displacements and inclinations cause crushing of the traditional joints, especially, towards the tip of the piles making it near impossible to seal.
(5) SPSP with traditional joints have low bending rigidity owing to vertical shear movements that occur at the joints under lateral load.
(6) Only one pile is installed at a time leading to unnecessary long construction periods and high operation costs.

With the backdrop of these numerous problems in SPSP with traditional joints, Kamon et al. (2001) assessed leachate migration paths in double wall SPSP applied as cutoff material in coastal waste disposal landfills. They proposed that a hydraulic conductivity of 10^{-8} cm/s is required of SPSP to effectively prevent leakage of leachate. To maintain this hydraulic conductivity over the whole SPSP wall, waterproof treatment of SPSP joints must be done to achieve hydraulic conductivity of the order 10^{-7} cm/s (Kamon et al., 2001). It is difficult to meet the required low hydraulic conductivity value using the traditional joints filled with mortar, Kimura et al. (2003) have therefore developed H-joint SPSP and proposed H-H joints to alternate in series with the H-joints. In this chapter, H-joint and H-H joint are described, evaluation of the hydraulic conductivity of H-jointed SPSP with H-H joints is done by experiments. Water-swelling sheets are used to seal the H-H joints.

2.2 Developed H-joint

Kimura et al. (2003) in an innovative contribution developed a new H-joint from a simple idea in which two steel pipe piles are connected by H-steel section welded on them as shown in Fig. 3. The H-steel section is what is referred to as the H-joint and will still have to alternate in series with the traditional joints pending development of another suitable joint. The connected piles are easily driven simultaneously by any of the existing pile driving methods. Among

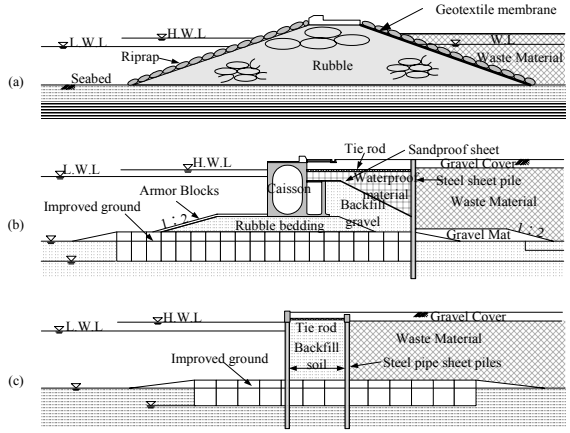

Fig. 1 Types of cutoff walls for coastal waste landfills commonly used in Japan

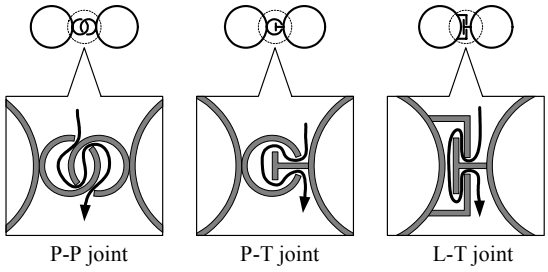

Fig. 2 Types of traditional joints with water-paths

advantages of H-joint piles are as follows:

(1) H-joint SPSP have high bending rigidity because H-steel section is welded rigidly and continuously against two steel pipes. Kimura et al. (2003) have shown by centrifugal modeling on rectangular H-joint SPSP foundations that H-joint SPSP exhibits higher lateral capacity than the SPSP with traditional joint connections.

(2) Precision of construction is high, with an accuracy of □3 mm in the horizontal direction; this is because one side of H-joint pile has flat-like shape that minimizes inclination of the pile during driving (Kimura et al., 2004).

(3) H-joint is completely water-proof because of the continuous welding, and can prevent backfill sand behind a seashore protection retaining wall from being washed away by water undercurrents.

(4) The use of the H-joint is environmentally friendly since it reduces the number of grouted joints.

(5) Two connected piles are driven simultaneously thus reducing the number of driven piles resulting in shortened construction period and reduction in operation costs (Kimura et al., 2004).

(6) The H-joint increases strength per unit length which means smaller foundation dimensions can be designed hence less amount of steel material is required.

Clearly, the H-joint satisfies permeability and bearing capacity requirements. The only point of contention is the fact that it will still alternate with the traditional joints. The authors are proposing H-H joint, described below, to alleviate this condition.

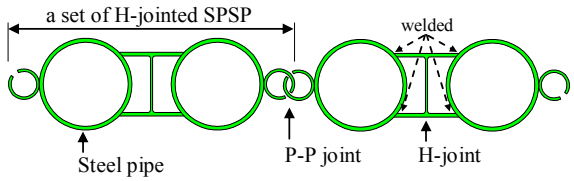

(a) H-joint alternating with P-P joint

(b) Photograph H-jointed SPSP

Fig. 3 H-joint SPSP

2.3 Proposed H-H joint

Traditionally, when H-joint SPSP is used as a vertical cutoff barrier, two adjacent H-joint SPSP is still continuously connected by traditional joint connection, such as P-P joint. Although the H-joint SPSP itself can exhibit complete impermeability, the risk of water leakage exists in the traditional P-P joint part between two H-joint SPSPs. Therefore, the authors have proposed "H-H joint", which is designed to use H-steel sections with different sizes to replace the traditional joint part between two H-joint SPSPs, as shown in Fig. 4. The H-H joint is formed from two H-steel sections of different sizes; their web heights and flange width sizes are such that the two H-steel sections just fit into one another. One H-steel section is welded on one side of a H-joint SPSP. Two such H-joint SPSPs are connected to form the H-H joint by driving a second SPSP adjacent to the first one so that their H-steel sections interlock. The H-H joint SPSP does not only maintain the advantages of H-joint SPSP, but also possesses enough waterproof property by using a water-swelling paint coated onto the H-H joint connection instead of filling mortar. That is, the H-H joint SPSP improves the joint part of two adjacent H-joint SPSP with a H-H steel joint connection, as a result, much more waterproof property than the traditional joint has been achieved. Furthermore, the steel ribs are installed in order to improve the tension resistance of the H-H joint connection, as shown in Fig. 4.

2.4 Permeability test on sealed H-H joint

The object is to evaluate the performance of H-H joint sealed by water-swelling paint sheet when exposed to 0.02 - 0.5 MPa water pressure in a coastal waste disposal facility; it is done by carrying out hydraulic conductivity tests. The thickness of the paint coat affects its swelling volume and the resulting swelling force; this determines waterproof strength of the paint at the H-H connection and therefore a suitable thickness of the paint coat that will produce required pressure resistance will be estimated.

The water-swelling paint swells when it comes in contact with water; it is a solid with fluidity blending of water-absorbing polymer, filling-agent, and fluxing material into synthetic-resin elastomer as

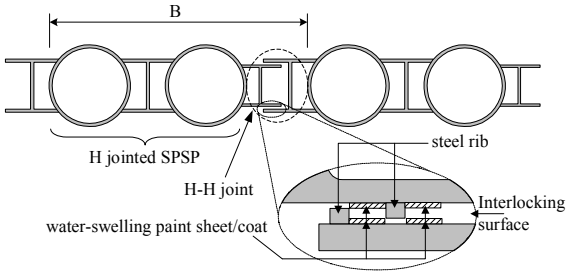

Fig. 4 The proposed H-H joint and slip restraining ribs

a base material. Water extracted from dried coating film of the water-swelling paint has been tested and found to satisfy the standard of water-purity based on the food hygiene law, and to suit the reduction of environmental impacts. The water-swelling paint used in the experiment begins to swell after 1 to 2 hours after it comes in contact with water, and the volume will be increased to about 20 times of the original volume after 24 hours achieving a hydraulic conductivity of 1.42 x 10^{-9} cm/s.

The H-H joint specimen was welded at the bottom and the sides of a 450 x 350 x 300 mm steel chamber shown in Fig. 5 so that water paths were only at the H interlocking surfaces. Rubber packing placed over the top of the chamber is for ensuring watertight conditions in the chamber. The steel plate is bolted over the rubber covered chamber. The influent flow and collected effluent flow was measured by the calibrated water reservoir and by weight using a weighing machine shown in Fig. 5, respectively.

In Japan, the specified standard hydraulic conductivity of waterproofing structures in coastal waste disposal landfills is 10^{-6} cm/s; it is based on hydraulic conductivity of a 50 cm thick soil layer. Since the current standard do not expressly specify standards for SPSP as cutoff walls in waste disposal landfills, the measured hydraulic conductivity of the SPSP are thus converted to equivalent hydraulic conductivity for an homogenous soil layer whose dimensions are equal to those used to develop the Japanese hydraulic conductivity (k ≤ 10^{-6} cm/s) standard as shown in Fig. 6.

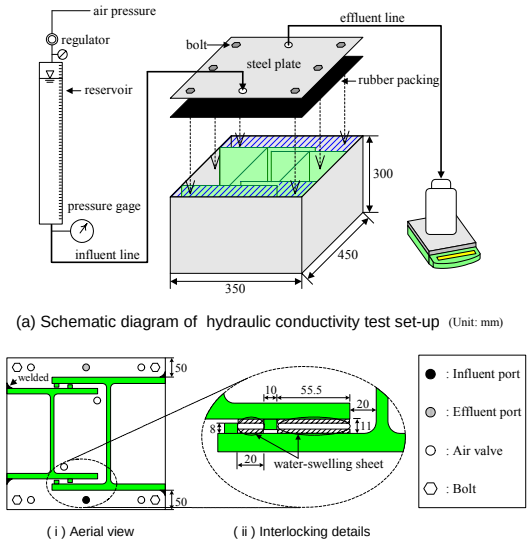

(a) Schematic diagram of hydraulic conductivity test set-up (Unit: mm)

(b) Schematic model aerial view and H-H joint interlocking details

Fig. 5 Hydraulic conductivity test layout, model aerial view and details of H-H joint interlock

2.5 Permeability of H-jointed SPSP with H-H joint

Figure 7 shows measured hydraulic conductivity for H-jointed SPSP with H-H joint sealed with water-swelling paint sheets of thickness 1, 2, and 3 mm against water pressure; also shown are equivalent hydraulic conductivity for P-T joints sealed by mortar and rubber (Oki et al., 2003). It is observed that k_e for H-H joints depends on water pressure; it increases with increasing water pressure, this may be because of the elastic nature of the water-swelling paint sheet. Paint sheets with thickness of 2 mm and above meet specified hydraulic conductivity of $k_e \leq 10^{-6}$ cm/s (Kamon and Inui, 2002) for water exclusion structures up to water pressures of 0.5 MPa. On the other hand a 1 mm paint coat meets the standard k_e of $\leq 10^{-6}$ cm/s up to a water pressure of 0.4 MPa.

In coastal waste disposal landfills, maximum water level difference between the contained water and the outer sea level must not exceed 2 m (Kamon and Inui, 2002); this level is controlled during heavy rains, water tide variations, and high water waves. Reports, however, indicate that some landfills have been filled to 5 m way beyond the specified limit of 2 m water level difference. It is important therefore to evaluate k_e of H-jointed SPSP with H-H joints for application as a cutoff material in waste disposal landfills based on the 5 m (equivalent to 0.05 MPa

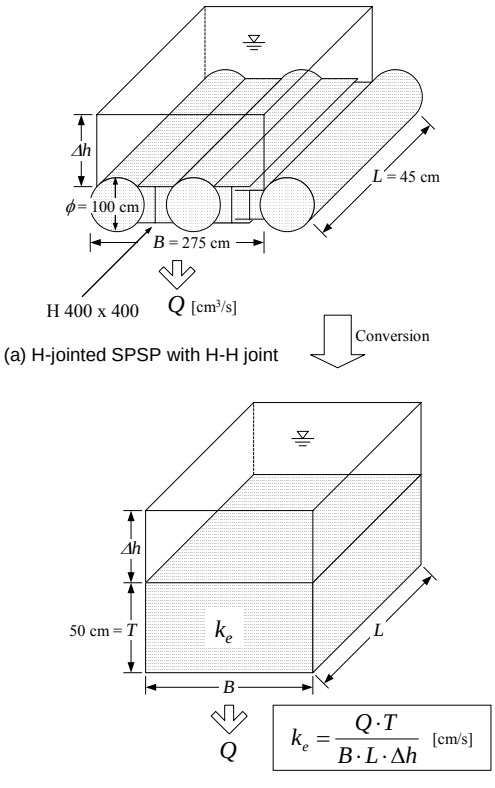

(a) H-jointed SPSP with H-H joint

(b) Equivalent homogeneous soil layer

Fig. 6 Conversion of the size of H-jointed SPSP with H-H joints into an equivalent homogeneous soil layer

water pressure) rather than the specified 2 m (equivalent to 0.02 MPa) water level difference.

From Fig. 7, k_e for H-H joints coated with 1 and 2 mm paint sheets was very low in the order of 10^{-8} cm/s at a water pressure of 0.05 MPa; k_e for the 3 mm paint coated joint was too small and could not be measured, since there was not effluent flow collected in the 6 hour test duration, k_e can be said to be below 1 x 10^{-9} cm/s. The authors propose use of $k_e = 10^{-8}$ cm/s in design of H-H joints sealed with this water-swelling paint.

When compared with findings of Oki et al. (2003), at 0.05 MPa the H-H joint has k_e of 2-order difference compared with the P-T joint sealed with mortar. The P-T joint sealed with mortar and rubber membrane is found to have $k_e = 10^{-8}$ cm/s like was the case with H-H joint, however, this value is based on laboratory findings in which application of mortar and the rubber membrane can easily be controlled; the case may not necessarily be true in actual construction practice because P-T joint treatment is done after construction and SPSP with this joint have low installation accuracy. Based on the advantages of the H-H joint SPSP mentioned in section 2.3 and backed by the measured low hydraulic conductivity values, the use of H-jointed SPSP with H-H joints sealed by water-swelling paint is highly recommended as a cutoff material in coastal waste disposal landfills, shoreline retaining walls, and in the construction of bridge pier SPSP foundation among other applications.

In this study the H-H interlock surfaces were sealed using water-swelling sheets, however, other methods of applying the water-swelling paint exist namely applying it in the form of paste. Unlike using a paint sheet which can easily peel off during construction, the pasted water-swelling material bonds more strongly with the steel material than the sheet type hence recommended.

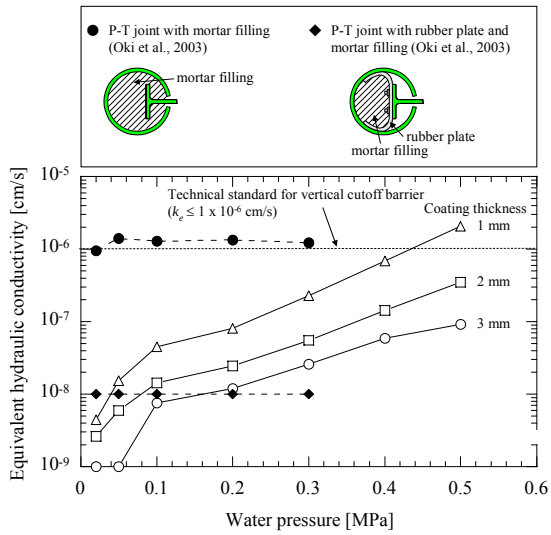

Fig. 7 Equivalent hydraulic conductivity versus resisted water pressure

3. Proposal of landslide susceptibility index in mountainous areas by using new technique, airborne laser altimetry

Shallow landslides have occurred in many locations contemporaneously by rainstorms, indicating that there is a kind of susceptibility that is characteristics to geology and geomorphology. We have successfully applied airborne laser scanning (ALS) technique to detect shallow landslides in granite and ignimbrite areas, of which results gives us a basis for the landslide-susceptibility evaluation in a wide area.

The areas investigated, Nishimikawa, Fukushima, and Hiroshima, experienced severe rainstorm-induced landslide disasters in 1972, 1998, and 1999 respectively, and ALS performed after the disasters extracted many old landslide scars before these disasters as well as new landslide scars that are clearly observed on aerial photographs after the events, indicating that these areas could have been recognized as susceptible areas to landslides before these disaster events. The landslide densities per square kilometers of slopes steeper than 20° in Nishimikawa granite area were 114 before the 1972 disaster and 293 by the 1972 event. The landslide density per square kilometers of slopes steeper than 20° in Fukushima disaster area was 117 per square kilometers before the 1999 disaster and 115 by the disaster. The landslide densities, which could be defined as above by using ALS, thus provide landslide susceptibility.

3.1 Case study for the 1998 Fukushima rainstorm hazard – Identification of shallow landslides and hazard assessment in an area of ignimbrite overlain by permeable pyroclastics–

We applied the airborne laser scanner technique to the Nishigo area of Fukushima rainstorm disaster that occurred from 26 to 31 August 1998 mainly by shallow landslide. More than a thousand landslides occurred on slopes of vapor-phase crystallized ignimbrite overlain by scoria, pumice, and ash. During the time of this disaster, five people were killed before dawn in a welfare house, which became a turning point for the Japanese government to establish a new law for the disaster prevention against slope movement hazard with the following disaster occurred in Hiroshima, western Japan in 1999.

We identified landslides during the 1998 disaster on aerial photographs with a scale of 1:8,000 and also by ground-truth geological investigation (Chigira, 2002; Chigira et al, 2002). Airborne laser scanning was performed for an area of 2.5 km^2 within the 1998 disaster area of Fukushima in late April, 2002. The system was ALTM1225. The ALTM sensor aboard a helicopter AS350B operated at 25000 pulses/s at a wavelength of 1064 nm with scanning angles 10 - 20°. This technique provides highly precise

horizontal (approximately 0.5 m) and vertical height locations (approximately 0.15 m). From the above data, 1-m grid DTM was made and a topographic map with 1-m contour interval was made.

(1) Geology and geomorphology

Small plateaus, about 60 to 100 m high above the nearby fluvial plains, occupy a wide area of Nishigo Village. The tops of the plateaus are essentially depositional surfaces of pyroclastic flow covered by thin tephra layers. The bedrock of the plateaus is the early Quaternary Shirakawa pyroclastic flow, overlain by thin beds of pyroclastics, which are thought to have erupted from Nasu volcano 200 to 350 thousand years ago. The Shirakawa pyroclastic flow has been divided into several flow units, and the flow in and around the investigated area has been fission track dated to 780 ka, and consists of dacitic ignimbrite (tuff), which is a weakly consolidated, massive, and intact tuff which had been subjected to vapor-phase crystallization. This vapor-phase crystallized tuff has characteristic weathering profile, which consists of hydrated, exfoliated, and disintegrated zones toward the ground surface (Chigira et al., 2002). The tuff of hydrated zone is significantly deteriorated but is still massive. The tuff of exfoliated zone is exfoliated to slope-parallel plates or lenses a few to 5 cm thick. The disintegrated tuff has lost its original rock structure and is soil-like.

The tephra layers overlying the Shirakawa pyroclastic flow are exposed in landslide scars and artificial cuttings; elsewhere they are covered by vegetation. These beds, which consist of mudflow deposits (diamicton made up of tuffaceous fines and andesite blocks) and air-fall deposits of scoria, pumice, and ash, are nearly horizontal, hence their outcrop traces fall along contour lines. The thicknesses of the mudflow deposits vary from 2 m to 20 m. The total thickness of the scoria and pumice beds varies from 0.5 m to 3.5 m, and the thickness of the ash occupying the top of the plateau is not precisely known but is estimated to be up to 10 m. The permeabilities of the underlying tuff is very low in comparison with the overlying tephra layers, which was one of the major causes of the landslides.

(2) Geomorphological and geological features of the landslides generated by the 1998 rainstorm and previous landslides

Aerial photographs taken from 10 to 11 September 1998 revealed that 203 landslides occurred within the laser-scanned area at the time of this disaster, but it is not easy to recognize whether previous landslide scars were present or not on the aerial photographs (Fig. 8A). Three dimensional images and maps made by laser scanner, however, clearly show previous landslide scars as well as those during this event (Fig. 8B, C). One hundred and two previous landslide scars are identified on the basis of

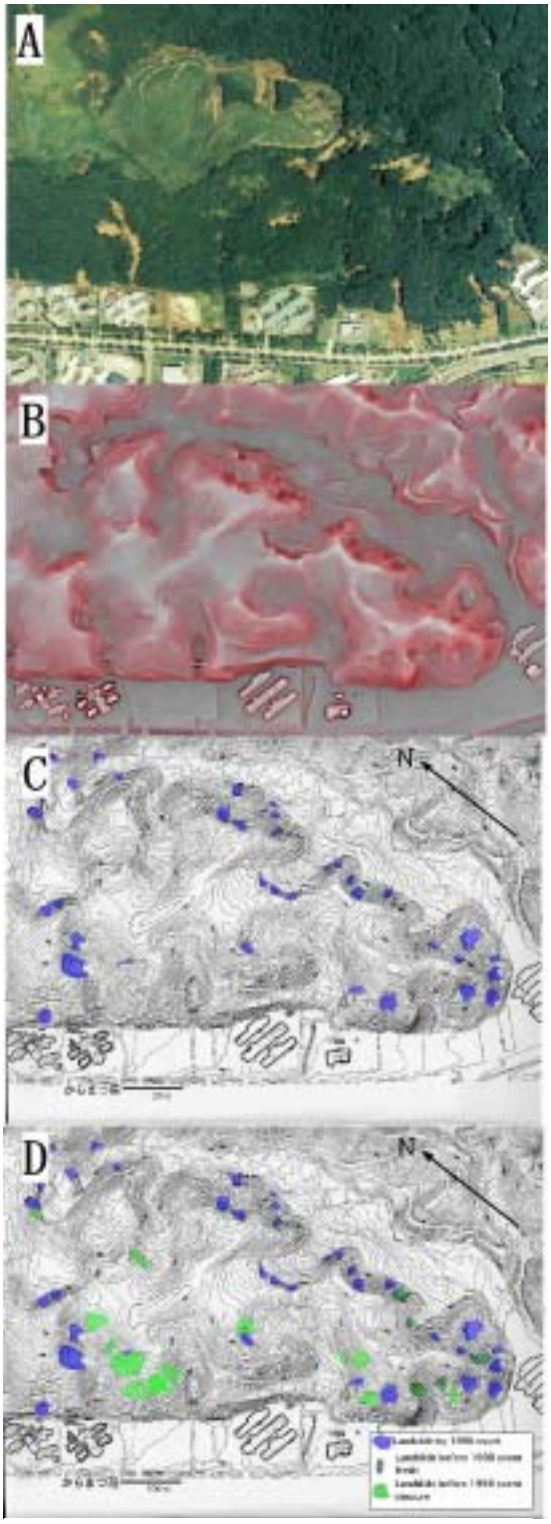

Fig. 8 Aerial photograph (A, Kokusai Kogyo, co.), three dimensional image (B Asia Air Survey co.), and maps (C and D) made by using airborne laser scanner, near the welfare facility, Taiyo no Kuni in Fukushima. Airborne laser scanner can identify previous landslides hidden by trees. Blue areas indicate landslide scars of 1998 event and green areas indicate landslide scars before this event. (Chigira et al., in preparation)

morphological characteristics, which will be described in the following.

As has been reported by Chigira (2002) and Chigira et al. (2002), three types of landslide occurred during this disaster. They are landslides of pyroclastic deposits overlying weakly consolidated ignimbrite, landslides of weathered tuff and colluvium, and landslides of depression fill. These types of landslide strongly reflected the hydrogeological structure. Typical morphology of these landslides is shown as laser-scanner maps and profiles in Fig. 9, in which profiles made by the laser scanner and by ground survey are both shown.
scanner and by ground survey are both shown.

1) Landslides of pyroclastic deposits overlying weakly consolidated ignimbrite

These landslides involved pyroclastic air-fall deposits overlying diamicton of mudflow deposits on weakly consolidated ignimbrite as well as debris on top. They were aligned along the trace of the air-fall deposits on gentle convex breaks along the periphery of the small plateaus. The hydrogeological structure, that is permeable beds overlies impermeable rock, effected the infiltrating behavior of rainwater: rainwater on small plateaus firstly infiltrates vertically and then flows laterally within permeable air-fall deposits and finally gushing out at the periphery of the plateaus to cause landslide.

The geometry of this type of landslide is clearly shown on a map made by laser scanner (Fig. 9A). The landslide scar of this type of landslide is an amphitheater or bowl-like depression and the ground surface along the path of debris transportation was essentially not eroded. The size of the bowl varies from 5 to 15 m in diameter and a few to 5 m in depth. Mudflow deposits usually are exposed at the bottom of the bowl, and air-fall deposits crop out in the upper part of the scar. The lower part of the bowl is very gentle and inclines from 5˚ to 15˚ and the upper part 30˚ to 45˚. The height of the head scarps varied from a few to 5 m.

2) Landslides of weathered tuff and colluvium

This type of landslide occurred on weakly consolidated ignimbrite with the sliding surface within the exfoliated zone, which forms the bottom of the intensively weathered zone (Chigira et al., 2002). This type of landslide stripped away most of the slide material, leaving bright-color rock surface of exfoliated zone at the landslide scar. The scars dip 25-45˚ with an average of 32˚, a few to 5 degrees steeper than the juxtaposing slope. The landslide scar itself is planar along the exfoliated zone (Fig. 9B), in contrast to the bowl-like morphology of the landslide scars of air-fall pyroclastics on the mudflow and the ignimbrite as is shown in contour maps and cross sections made by the air-born laser scanner. In comparison with the cross section made by ground survey, the cross section made from laser scanner gives somehow rounded edge of the top of landslide scar, but the shape of landslide scar is generally clearly detected. The size of the scar varies from 5 to 30 m in width and length and less than a few meters in the depth.

3) Landslides of depression fill

The intense rainfall also triggered failure of colluviums or ash that filled depressions, although this type of failure seemed less common than the other two types. A typical example of this was a landslide that occurred near Daishin Junior High School, 15 km northeast of Taiyo-no Kuni, where the landslide, leaving a scar 5 m deep and 80 m long, exposed a former buried stream again. The hollow

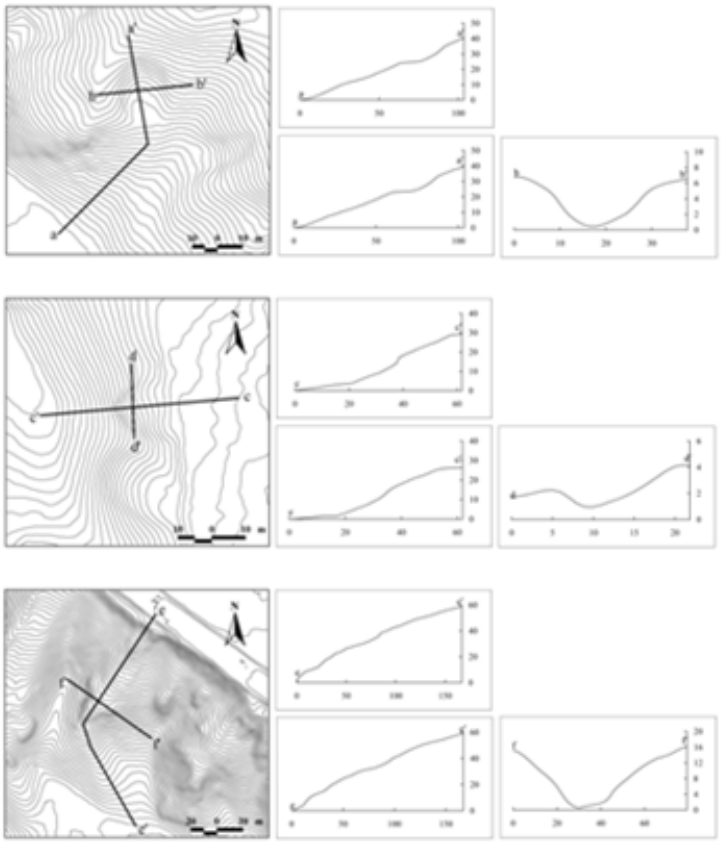

Fig. 9 Laser scanner maps and profiles of three types of landslides that occurred in Nishigo village by the 1998 disaster (Chigira et al., in preparation). Contour interval is 1 m. Top: Landslides of pyroclastic deposits overlying weakly consolidated ignimbrite; middle: Landslides of weathered tuff and colluvium; bottom: Landslides of depression fill. Upper left profiles are made by ground survey.

upslope of this landslide had old depressions a few meters in diameter and less than 1 m deep, indicating that underground erosion and ground settlement preceded the landslide. The gradient of this hollow before the slide is assumed to be 15° from the following survey. In addition, this old depression fill was cut artificially for construction at the lower part of the slope and this landslide seems to have started at this cutting.

Fig. 9C shows the laser scanner map of this type of landslide. Two landslides of depression fill occurred on slopes above knick points of hollows located at the heads of ravines, retrogressing the knick points upslope (cross section of Fig. 9C). The gradients of the slopes with underground erosion awere 12° and 15° .

3.2 Granitic rock areas

Granitic rocks have been experiencing many landslides by rainstorms in Japan (Fig. 10, Chigira, 2001). We applied airborne laser scanner to Obara village, central Japan, where devastating disaster occurred by large number of landslides during the rainstorm with the precipitation of 238 mm per 6 hours in July 1972. By examining the map in comparison with the aerial photographs taken after the disasters, we identified many landslide scars that occurred at the time of the disaster (Fig. 11, Tobe and Chigira, 2004). We also recognized many old landslide scars that had already existed at the time of the disasters but had been difficult to identify in aerial photographs. This ALS landslide map and geologic map that we made by intensive field survey clearly showed the strong control of landslide density by rock types as has been reported by Yairi et al. (1973). The landslide densities per square kilometers of slopes steeper than 20° were 114 before the 1972 event, 293 by the 1972 event, and 408 altogether, respectively.
Corresponding landslide densities in granodiorite area were 28, 13, and 41. These numbers clearly indicates that we could have known that this granite area is very susceptible to landslide.

3.3 Areal susceptibility evaluation from the airborne laser scanner

As has been described, airborne laser scanner performed under the good condition, say less tree leaves, can identify old landslides while aerial photographs can only detect new landslides if they are not large. The occurrence of an old landslide is hard to be dated, but landslide distribution for long periods records the susceptibility of a given area against landslide. For example, Fukushima disaster area had a landslide density of at least 117 within one km2 of slopes steeper than 20 degrees before the 1998 event and had a new landslide density of 233/km^2 at the event. These numbers are quite large and on about the same order of the landslide density of devastating disaster that occurred in weathered granite area of Obara village, central Japan, which had a landslide density of 294/km^2 at the event and at least 114/km^2 before the event (Tobe and Chigira 2004; Duan et al., in preparation). The repetition of shallow landslides must be closely related to the rate of production of slide materials, that is mainly by weathering, but constantly high landslide density suggests high susceptibility.

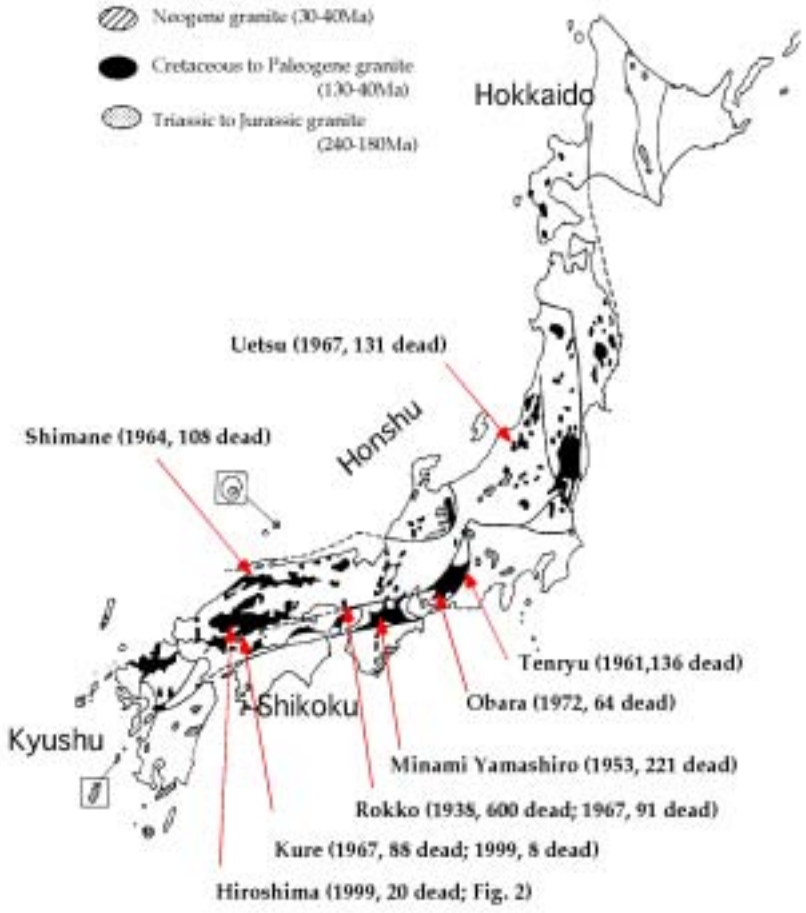

Fig. 10 Landslide disasters in granitic rock areas (Chigira, 2001)

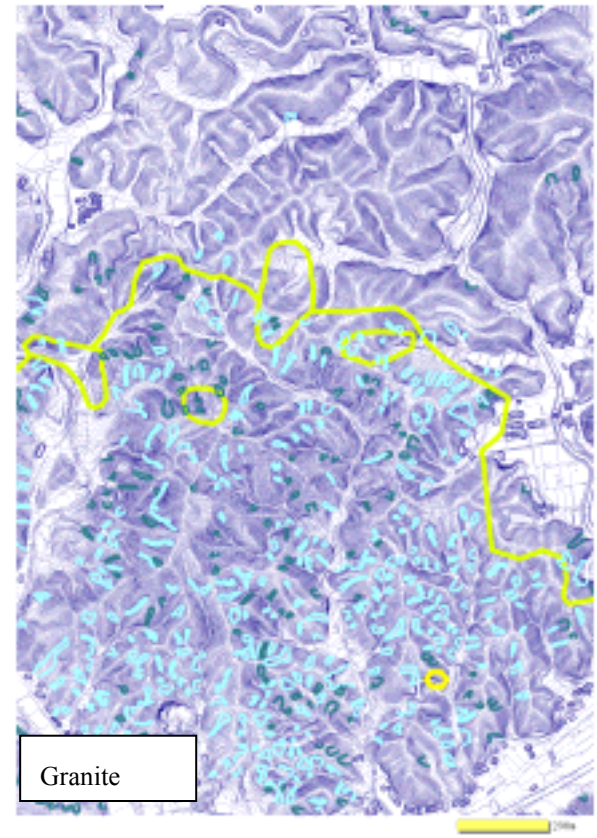

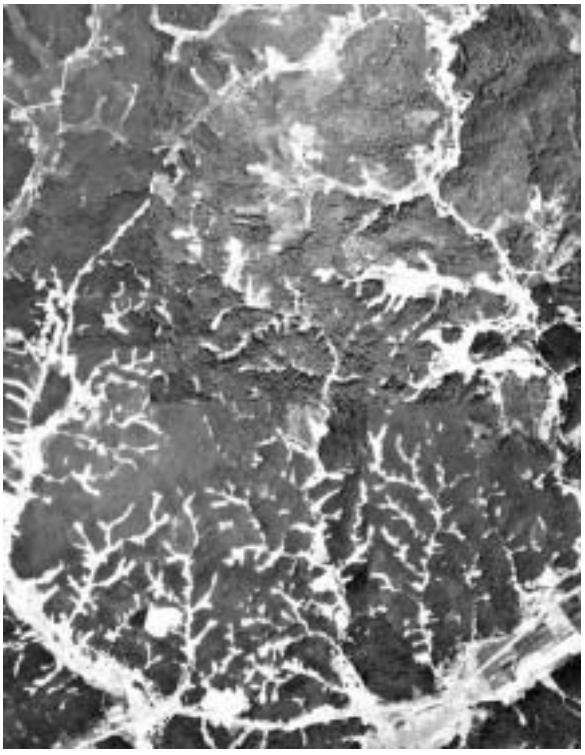

Fig. 11 Laser scanner map in Obara village (upper) and aerial photograph of the same area (lower, Aero Asahi Co.). Landslides in blue color are by the 1972 disaster event and those in green color are previous ones. (Tobe and Chigira, 2004)

4. Landslide hazard prediction in residential areas of hillside

4.1 Neural-network for hazard mapping of valley fills

(1) Background

Recent destructive earthquakes in urban regions, such as the 1978 Miyagiken-oki earthquake, the 1993 Kushiro-oki earthquake and the 1995 Hyougoken-nanbu earthquake, have triggered landslides in many gentle slopes of residential areas around Sendai, Kushiro, Nishinomiya and Kobe. The earthquake-induced slope instability that has occurred is closely related to these artificial landforms, especially valley fills (embankments). More than 60% of the unstable slopes in the Kobe-Nishinomiya urban region are in artificial valley fills. This instability was caused by strong ground movements during the 1995 Hyougoken-nanbu earthquake.

Investigation of past artificial landform changes and multi-variate analysis of case studies of past earthquake disasters show that differences in the shape of fills, such as depth, width, inclination angle of the base, and cross-sectional form, may be the key discriminating factors of slope instability.

Triggering mechanisms (e.g. earthquakes) need to be considered in the analysis for accurate estimation, however, it is difficult to include earthquake parameters in such linear multi-variate analysis (quantification theory II). Neural network analysis is applied to assess large fill slope instability in urban residential areas.

(2) Neural network model

The developed neural network model includes both causative factors (shape of fills, groundwater condition, age of construction) and the triggering factors (distance from the fault, moment magnitude, direction to fault). The model consists of nine input factors, twelve intermediate neurons, and two output items (stable or unstable) as shown in Figure 12. Back propagation method (BP method) was used to investigate most appropriate set of the weight of connections between the three layers of the model. The control parameters of BP method, learning ratio, number of intermediate neurons, and number of learning times, were determined to minimize the total error between the input and the out put.

Summation of square of weight between input layer and intermediate layer represents the power of influence of input factors. Each sum of square of weight divided by total sum of square of weight should be used as percentages contributed of the input factors. The thickness of fills and direction to fault are the first (29.9%) and second (16.1%) contributing factors as shown Table 1.

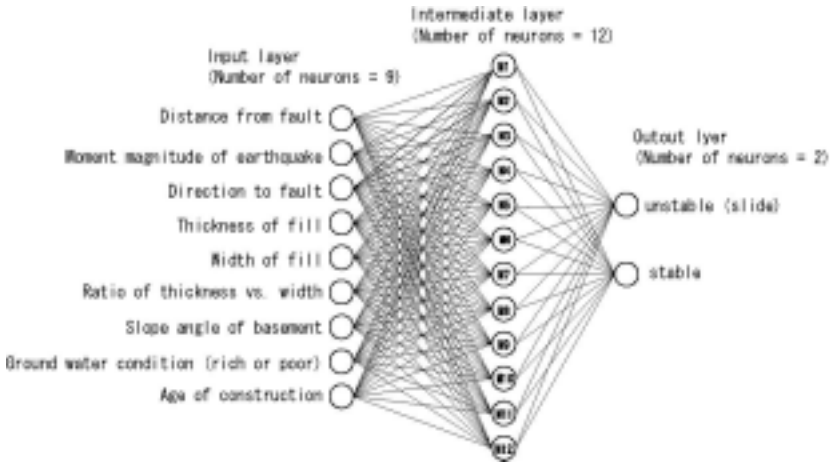

Fig. 12 Neural network structure of the prediction model

Table 1 Weight of bonds between input layer and intermediate layer (M-1～12:neurons of intermediate layer)

	Distance from fault	Mw	Direction to fault	Thickness	Width	Width／Thickness	Slope of base	ground water	Age	Threshold
M-1	-1.53	-2.07	0.40	-0.15	-0.38	-1.15	-0.68	2.08	-1.24	1.41
M-2	-2.84	-2.21	11.40	-6.36	-13.14	-2.93	1.36	2.81	0.61	6.85
M-3	8.38	-11.81	10.89	-29.19	-4.52	8.35	-15.60	-1.78	6.03	7.59
M-4	-20.32	-13.44	6.69	-31.00	30.35	18.55	-7.04	8.09	-6.28	-6.25
M-5	3.57	2.32	-23.46	-3.56	8.09	2.82	2.70	13.02	2.05	3.79
M-6	-3.82	-1.23	4.90	6.01	7.18	-5.69	3.48	7.47	-8.09	-3.90
M-7	-14.51	-7.32	17.10	-25.52	-8.85	8.84	6.31	2.79	-0.06	-12.09
M-8	-0.79	-1.23	2.08	0.78	1.20	0.51	-0.01	1.34	-0.41	2.14
M-9	-0.43	-0.31	22.30	6.39	5.40	6.24	-7.88	-1.98	2.31	-2.94
M-10	12.56	2.75	-11.39	-16.22	1.36	9.73	19.11	4.26	0.84	2.93
M-11	-11.93	16.15	10.94	6.21	-13.26	-1.18	20.14	0.31	1.00	-0.72
M-12	-16.27	-5.03	-9.05	28.25	-3.46	-24.92	-0.64	6.35	-9.78	1.45
Sum of square of weight	1297.24	690.92	1993.43	3695.11	1530.00	1300.62	1187.93	378.64	279.96	
Power of influence (%)	10.6	5.6	16.1	29.9	12.4	10.5	9.6	3.1	2.3	

Table 2 Ratio of correct interpretation by the neural network analysis

			Learning		Identifing
			for All	for Evaluation	for Evaluation
Ratio of correct answers (%) (Correct answers／Total)	Total		97.1 (305/314)	95.3 (204/214)	92.0 (92/100)
	Earthquakes	1995Kobe	97.3 (249/256)	95.1 (174/183)	94.5 (69/73)
		1978Miyagiken-oki	96.3 (52/54)	96.3 (26/27)	85.2 (23/27)
		1993Kushiro-oki	100 (4/4)	100 (4/4)	-

(3) Results of the analysis (learning process)

Table 2 shows results of neural network analysis, that are number of samples using analysis, number of samples given correct answers, and ratio of correct interpretation. The ratio of correct interpretation higher than 90 % means high accuracy for detection of instability of fills by strong earthquake motion.

(4) Sensitivity analysis

The developed neural network model was independently checked against another data set (not used in the learning process) and sensitivity analysis was conducted. The results of analysis on the independent data set show the high accuracy of the model remains the high ratio of correct interpretation even less comparing to the results of learning process.

The dependence between each input factors and output value was investigated by sensitivity analysis. Value of a selected input factor changes gradually during that value of the other input factors were hold in average value. As shown Figure 13, instability of valley fill increases in the shape of less than 5 m in thickness, wider than 60 m, larger than 20 of ratio of thickness vs. width, steeper than 15 degrees of base angle at central part of valley, and the axis of valley

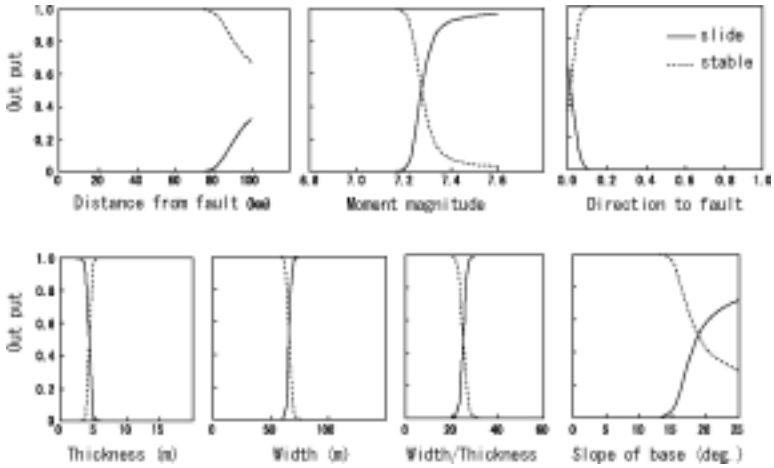

Fig. 13 Results of sensitivity analysis

perpendicular to fault. Earthquake greater than 7.2 of magnitude, and earthquake more than 80 km far from valley fill increase instability of the fill.

(5) Performance evaluation of the model

The three major earthquakes in 2003, the Miyagiken-oki earthquake in 26 May, the Miyagiken-hokubu earthquake in 26 July, and the Tokachi-oki earthquake in 26 September, should evaluate the performance of the developed model. Eight fills in northern part of Miyagi prefecture including five stable cases were investigated by using high precision surface wave exploration and dynamic penetration tests (mini SPT tests). The N-value of the mini SPT calibrated the results of the surface wave exploration (S-wave velocity).

The shape of valley fills determined by the cross section of S-wave velocity of each fills was made as input data to the model. The seven fills including four stable cases were classified correctly; one stable case was classified to be unstable one (incorrect answer) by using the developed model. Thus, the fine performance and high reliability of the model was shown in disasters by the two northern Miyagi earthquakes.

case of the Tokachi-oki earthquake will be resulted from the unexpected conditions of input factors that are the both type of movement and earthquake. These performance evaluations of the model suggest that instability mechanism should be studied to be beyond analysis of experiences including the neural network analysis.

(6) Application to hazard mapping

The neural network analysis appears to have advantages over the multi-variate analysis because the neural network model can represent a kind of non-linear regression model to be fine performance with limited number of samples (experiments) even in complicated cases. The newly proposed neural network model can consider the triggering factors (earthquake parameters) for each expected rupture of faults. It means that the hazard mapping of valley fills in urban residential areas should be possible to conduct by using the neural network model.

Figure 14 shows a result of hazard mapping of valley fill type landslides in Tokyo-Yokohama district.

More than half of the fill-slopes should be classified into a high-risk group. The regional difference of risk

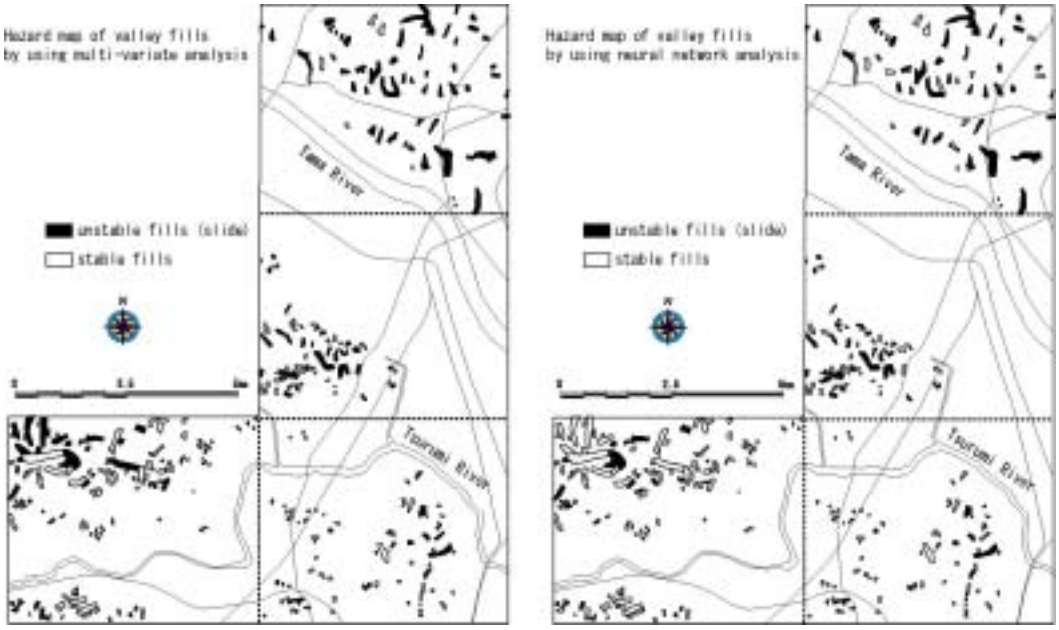

Fig. 14 Maps showing the results of the stability assessment of valley-fill type landslides in Tokyo-Yokohama district by using both the multivariate analysis and the neural network analysis

Several fills developed in Sapporo and Kushiro urban regions became unstable by the Tokachi-oki earthquake. The developed model checked the four cases of these, however, all of them were interpreted incorrectly. Cases in Sapporo were strongly related to liquefaction of limited shallow part of large valley fill, and the landslide in Kushiro occurred in the part of large fill slope (not to be valley-fill type). The distance from the rupture zone of the Tokachi-oki earthquake was over 100 km at the both cities. It means that the poor performance of the model in the

on the fill-slope landslides is obviously depends on geology. Vertical elevation drop between alluvial plain and terrace surface controlled the depth of valleys in this district. Shallow dissected valleys developed widely in the northern part from the Tama River (named the Musashino terrace) that is lower (younger) than the terraces in southern part (named the Shimo-sueyoshi terrace, the Tama hills). Valley fills in the Musashino terrace are shown in high-risk compared to the fills in southern part because of its shape of valley fills.

The landslide potential by heavy rainfall in Tokyo-Yokohama district such as shallow collapse of soft material on seep slopes of the Kanto Loam will decrease by the effects of protection works from 1970's that have still continued by the Government. However, the risk at the earthquake, especially by the artificial valley fill type landslide, still remains, and increases by the continuous human activity in this district. It is thought that the loose and uncompacted material of filling slopes with poor drainage systems is responsible to the occurrence of the landslides. Landslides associated with artificial valley fills will be common in Tokyo-Yokohama district at the next large earthquake disaster (2xxx Tokyo earthquake). Many cities in Japan have almost the same conditions at risk of urban landslides such as the Hanshin district and Tokyo-Yokohama district; where, there is some significance to conduct hazard mapping on the potential of urban landslide disaster.

4.2 Effects of duration of rainfall on landslides

Several damaging landslides and debris flows on July 20, 2003, in southern Kyushu, Japan, attracted international attention and resulted in one of the major natural disasters of recent years. Large amounts of rain fell on July 19-20 as a Baiu front passing over the Sea of Japan met a high-pressure zone moving up from the southeast over the Pacific Ocean. Altogether, 21 lives were lost related to the sediment disasters and more than 240 homes were either damaged or destroyed by landslides, debris flows and flooding. Nevertheless, such natural disasters related to landslides and debris flows occur frequently in Japan and local residents generally acknowledge their potential exposure to these hazards, but risk and vulnerability may be complicated by other social and economic factors.

Initial news reports following the July 20th storm suggested that only a few slope failures occurred. While all fatalities occurred in two debris flows in Minamata (Hogawachi and Fukagawa) and a landslide in Hishikari, damage by mass movements was widespread in southern Kyushu. In the most impacted areas of Minamata (4 km^2) and Hishikari (2 km^2), 37 and 14 landslides were identified, respectively. Almost all landslides in the Minamata-Hishikara region were underlain by weathered andesite, tuff-breccia, and tuff, and the slope gradients of 20 inspected landslides were generally only moderately steep (initiation zone 20 – 38°). None of the debris flows that were examined in the channels appeared to initiate as debris flows, nor did they rapidly convert from landslides to debris flows as has been suggested in other studies [Fannin and Rollerson, 1993; Iverson et al., 1997]. Deeper landslides typically traveled further downslope if gradients were steep and often developed into debris flows. Rainfall intensities during the 2- and 6-h periods up to and including the time of most damaging landslides at Hishikari and Minamata were very intense – 53 and 89 mm h^{-1}, respectively. Total storm precipitation prior to failure was very high at Hishikari (< 337 mm; ≈ 3.5 km west of the fatal landslide), but not extraordinary in Minamata (< 265 mm; ≈ 2 km from the two major debris flows). Only moderate rainfall occurred at Hishikari and Minamata on the day prior to the disasters and antecedent 10-day rainfall was only 75 and 70 mm, respectively.

For the largest and most damaging landslide/debris flow at Minamata (Figure 15), it appears that pore water pressure likely developed at the base of the weathered andesite within the limited space in a system of interconnected fractures and interstices. This probable scenario of rapid pore pressure accretion and subsequent slope failure of the relatively deep regolith is in contrast to theoretically derived responses in homogenous porous media, which suggest that thin soil mantles become unstable during short-term, high-intensity storms, while deeper regoliths fail during prolonged storms of moderate intensity [e.g., Haneberg, 1991]

Fig. 15 Landslide and debris flow at Hogawachi in Minamata, Kyushu, on 20 July 2003; 15 people killed and 13 homes destroyed.

5. Conclusions

Methodologies for assessing vulnerability to the geo-hazards, and techniques for improving the performance of geotechnical works in urban areas are investigated. Major results obtained from this study may be summarized as follows.

(1) Steel sheet pile walls for retaining waste fill in

waterfront areas should meet the performance requirements that should be structurally stable as well as prevent the pore water migration through the wall. A new technique using the steel joint, called H-H joints, is proposed.

(2) Airborne laser scanning (ALS) technique achieves high precision in detecting shallow landslides in granite and ignimbrite areas. Since these shallow landslides occur repeatedly within a period of 100 years, density of landslides per unit area obtained by the ALS technique can be a good susceptibility index of landslides.

(3) Neural-network technique is applicable to the prediction of failures in valley fills during earthquakes.

(4) Some of the large damaging landslide/debris flow, such as those at Minamata in 2003, may be caused by the pore water pressure developed at the base of the weathered andesite within the limited space in a system of interconnected fractures and interstices.

Acknowledgments

This paper summarizes the results of the COE research performed by Geo-disaster Division, DPRI. Primary part of this paper, i.e. Chapters 2 through 4, is based on the contributions by the 2nd through 5th authors. The first author compiled the paper as project leader in 2003. The research presented in Chapter 2 was performed under the supervision of Prof. Makoto Kimura, Graduate School of Engineering, Kyoto University and Prof. Masashi Kamon, Graduate School of Global Environmental Studies, Kyoto University. The authors wish to express their sincere gratitude to these professors.

This research was supported by the Japanese Ministry of Education, Culture, Sports, Science and Technology (MEXT) 21st Century COE Program for DPRI, Kyoto University (No.14219301, Program Leader: Prof. Yoshiaki Kawata) as well as the Grant-in-Aid for Scientific Research (B) (2) (No. 15310129, Principal Investigator: T. Kamai, Kyoto University). This manuscript partly follows the instructions given in IAHS Press (1995). The study in Chapter 3 was also funded by the Ministry of Education, Culture, Sports, Science and Technology (MEXT) (Special Coordination Fund for Promoting Science and Technology, Aereal Prediction of Earthquake and Rain Induced Flow Phenomena (APERIF Project), Principal Investigator: Kyoji SASSA) and the Japan Landslide Society.

References

Chigira, M. (2001): Micro-sheeting of granite and its relationship with landsliding specifically after the heavy rainstorm in June 1999, Hiroshima Prefecture, Japan. Engineering Geology. 59, 219-231.

Chigira, M., (2002): Geologic factors contributing to landslide generation in a pyroclastic area: August 1998 Nishigo Village, Japan. Geomorphology 46, 117-128.

Chigira, M., Duan, F., Yagi, H., and Furuya, T. (in preparation) Identification of shallow landslides and hazard assessment in an area of ignimbrite overlain by permeable pyroclastics by using airborne laser scanner – Case study for the 1998 Fukushima rainstorm hazard –

Chigira, M., Nakamoto, M., Nakata, E., (2002): Weathering mechanisms and their effects on the landsliding of ignimbrite subject to vapor-phase crystallization in the Shirakawa pyroclastic flow, northern Japan. Engineering Geology 66, 111-126.

Duan, F. and Chigira, (in preparation) Mapping shallow landslide and evaluating slope stability using digital terrain analysis with high resolution DTM data

Fannin, R.J., and T.P. Rollerson, (1993):Debris flows: some physical characteristics and behaviour, Can. Geotech., J. 30, 71-81.

Haneberg, W.C. (1991): Pore pressure diffusion and the hydrologic response of nearly saturated, thin landslide deposits to rainfall, J. Geol. 99, 886-892.

Iverson, R.M., M.E. Reid, and R.G. LaHusen, (1997): Debris-flow mobilization from landslides, Annu. Rev. Earth Planet. Sci. 25, 85-138.

Kamai,T., and H. Shuzui. (2002): Landslides in urban region, Riko-tosho, 200. (in Japanese)

Kamai, T., Shuzui, H., Kasahara, R., and Y. Kobayashi, (2004): Earthquake risk assessments of large residential fill-slope in urban areas, Landsides – Journal of the Japan Landslide Society, 157, 29-39 (in Japanese)

Kamon, M. and Inui, T. (2002): Geotechnical problems and solutions of controlled waste disposal sites, Journal of Geotechnical Engineering, JSCE, No.701/III-58:1-15 (in Japanese).

Kamon, M., Katsumi, T., Endo, K., Ito, K, and Doi, A. (2001): Evaluation of the performance of coastal waste landfill with sheet pile containment system, Proceedings of the Fourth Japan National Symposium on Environmental Geotechnology, 279-284 (in Japanese).

Kimura, M., Too, A.J.K., Inazumi, S., Isobe, K., and Nishiyama, Y. (2004): Innovative development of steel pipe sheet pile joint, Proceedings of the Third Civil Engineering Conference in the Asian Region, submitted.

Kimura, M., Too, A.J.K., Isobe, K., and Nishiyama, Y. (2003): Offshore construction of bulkhead waste facilities by H-joint steel pipe sheet piles, Proceedings of BGA International Conference on Foundations: 'Innovations, Observations, Design and Practice', 443-452.

Oki, T., Torizaki, K., Kita, H., Yoshida, M., Sakaguchi, Y., and Yoshino, H. (2003): Evaluation of impermeability performance of the vertical impermeable walls by using steel sheet piles and steel pipe sheet piles, Proceedings of the Fifth Japan

National Symposium on Environmental Geotechnology, p53-58 (in Japanese).
Tobe, H. and Chigira, M. (2004) Relationships between landslide densities detected by airborne laser scanner and the petrological texture of granitic rocks. to be presented at the International Geological Congress, Florence, Italy.
Yairi, K., Suwa, K., Masuoka, Y. (1973) Landslides by the rainstorm of July 1972 Obara Village and Fujioka Villate, Nishikamo, Aichi Prefecture. Yano, K. ed. Report of the Grant-in Aid for Scientific Research from the Japanese Ministry of Education, Science, Culture and Sports. 92-103. (in Japanese)

要　旨

低平地を中心として急速に周辺丘陵地へと拡大する都市域では，地震時液状化，宅地造成地盤崩壊，人工･自然斜面崩壊など，地盤災害の危険性が増している。本研究は，これらの地盤災害に対する都市域の脆弱性診断技術と危険度評価技術の高度化，地盤基礎構造物の性能向上技術の開発を目的とする。平成15年度のとりまとめとして，本論文では，廃棄物埋立護岸の環境脆弱性と性能向上，レーザースキャナー技術を用いた山地での表層崩壊発生危険度評価の提案，丘陵地斜面における地すべり災害の予測モデルの開発についてとりまとめた.

キーワード: 環境，危険度評価，丘陵地，山地，地盤災害

COE

都市および周辺地域における地盤災害予測とハザードマップに関する研究

井合　進，稲積真哉，千木良雅弘，釜井俊孝，Sidle, R.C.
三村　衛，諏訪　浩，斉藤隆志，飛田哲男

１．はじめに

低平地を中心として急速に周辺丘陵地へと拡大する都市域では，地震時液状化，宅地造成地盤崩壊，人工・自然斜面崩壊など，地盤災害の危険性が増している。本研究は，これらの地盤災害に対する都市域の脆弱性診断技術と危険度評価技術の高度化，地盤基礎構造物の性能向上技術の開発を目的とする。平成１５年度のとりまとめとして，本論文では，廃棄物埋立護岸の環境脆弱性と性能向上，レーザースキャナー技術を用いた山地での表層崩壊発生危険度評価の提案，丘陵地斜面における地すべり災害の予測モデルの開発についてとりまとめた.

2. 廃棄物埋立護岸の環境脆弱性評価と性能向上

海面埋立処分場における埋立護岸は、廃棄物、建設発生土、および浚渫土砂の海面埋立処分に対応して、港湾保全との整合を図りつつ、埋立処分する空間を確保するためのものである。廃棄物埋立護岸は、波浪、高潮、津波など海上特有の諸条件に対して十分安全であるとともに、廃棄物からの浸出水が海域へ流出することのない構造でなければならない。近年では、施工効率や経済性を考慮して、鋼管矢板を用いた廃棄物埋立護岸が採用されている。本研究では、既往の鋼管矢板護岸における継手箇所の問題点に着目し、遮水性能に関する課題を明らかにした。さらに、実海域における鋼管矢板の施工性や遮水性向上に貢献し得る H-H 継手を介した連結鋼管矢板の性能を透水試験によって評価し，H-H 継手を介した連結鋼管矢板の適用が効果的であることを明確にした。

3. 山地での表層崩壊発生危険度評価指標の提案 ―レーザースキャナー技術を用いて―

表層崩壊は，個々の規模は小さくても広い範囲に多数発生することが多く，それが引き起こす災害は甚大になることが多い。表層崩壊に対して危険な斜面を広い地域から抽出することは，地盤の多様性のために難しいが，広い範囲の危険度を評価することは可能になりつつある。我々は，地質特性とレーザースキャナー地形計測技術を用いて地域の表層崩壊危険度を評価する新たな手法を開発した。レーザースキャナー計測は，航空機から地表に向けてレーザーパルスを発射し，樹間を通過して返ってくる反射をとらえ，地表を精密に測量する技術である。

本研究では，1972 年西三河災害箇所および 1998 年福島県南部豪雨災害箇所に，レーザースキャナー計測を適用した。その結果，花崗岩地域で崩壊が密集して発生したことと，花崗閃緑岩地域では崩壊が極めて少なかったことが明確になり，災害前にレーザースキャナー計測が実施されていれば，花崗岩地域の崩壊危険性の高さを数値的に推定可能であったことが明らかになった。

上述のように，レーザースキャナー計測によって，100 年オーダーの期間に発生した崩壊密度を読み取ることが可能であり，この崩壊密度は，特定地域の崩壊危険度インデックスとして用いることができると考えられる。今後，崩壊跡の持続時間と崩壊の免疫期間や植生のレーザースキャナー計測結果への影響について検討することによって，この実用化をはかることができる。

4. 丘陵地斜面における地すべり災害の予測モデルの開発

丘陵地斜面における地すべり災害の予測について、新たな予測モデルの開発とケーススタディを行った。１９７８年宮城県沖地震、１９９３年釧路沖地震、１９９５年兵庫県南部地震等、都市に被害を与えた地震では、人口密集地に形成された多数の宅地盛土（多くは谷埋め盛土）が、大規模に変動（地すべり）した。そこで、谷埋め盛土の変動・非変動事例 314 例について，ニューラルネットワークを用いた変動予測モデルを構築した。モデルの感度解析及び未学習データを使用した精度評価試験を行った結果、いずれにおいても良好な成績を得た。また、２００３年の水俣災害の発生メカニズムについて検討し、深部における間隙水圧の全般的な上昇が、表層崩壊の急激な発生をもたらした原因であることを明らかにした。